Relativistic theory for localized electrostatic excitations in degenerate electron-ion plasmas

Michael Mc Kerr
Center for Plasma Physics, Department of Physics and Astronomy, Queen's University Belfast, BT7 1NN Northern Ireland, UK

Fernando Haas
Instituto de Física, Universidade Federal do Rio Grande do Sul, 3308-7286 Av. Bento Gonalves 9500, Porto Alegre, RS, Brazil

Ioannis Kourakis
Center for Plasma Physics, Department of Physics and Astronomy, Queen's University Belfast, BT7 1NN Northern Ireland, UK

A self-consistent relativistic two-fluid model is proposed for electron-ion plasma dynamics. An one-dimensional geometry is adopted. Electrons are treated as a relativistically-degenerate fluid, governed by an appropriate equation of state. The ion fluid is also allowed to be relativistic, but is cold, non-degenerate and subject only to an electrostatic potential. Exact stationary-profile solutions are sought, at the ionic scale, via the Sagdeev pseudopotential method. The analysis provides the pulse existence region, in terms of characteristic relativistic parameters, associated with the (ultra-high) particle density.

I. INTRODUCTION

A detailed understanding of the physics of dense plasmas in one-dimensional (1D) geometry is becoming increasingly important, both for practical and fundamental reasons [1]. For instance, 1D dense plasmas are of relevance to the target normal sheath acceleration mechanism [2] produced during the irradiation of solid targets with a high-intensity laser available with coherent brilliant X-ray radiation sources [3]. Furthermore, the nonlinear dynamics of 1D degenerate plasmas shows a rich variety of behavior; applications include the dense quantum diode [4], the electron-hole plasma injected into quantum wires [5], the 1D fermionic Luttinger liquid [6], breather-mode oscillations in 1D semiconductor quantum wells [7], Lagrangian structures in dense 1D plasmas [8], 1D nonlinear envelope modes in dense electron-positron-ion plasmas [9], among others. Sagdeev's pseudopotential method was used to study the propagation of wave-structures of arbitrary amplitude in a relativistically-degenerate electron-positron-ion plasmas in Ref. [10], making use of Chandrasekhar's relativistic 3D equation of state within a non-relativistic 1D geometry. Small-amplitude nonlinear structures in dense, relativistic electron-positron-ion plasmas have also been investigated by means of hydrodynamical modeling and a multiple-scale perturbative method in Ref. [11]. In addition, systems in the presence of a strong magnetic field have a modified mobility of the charged carriers due to confinement in the direction along the field, thus effectively behaving as a one-dimensional gas. In this context, relativistic dense one-dimensional plasmas are realized in e.g. the atmosphere of neutron stars [12–14].

Due to the high densities considered for this class of systems, the large value of the Fermi momentum demands the inclusion relativistic effects. In this case, the relativistic parameter [15] given by p_F/mc is not negligible, where p_F and m are respectively the Fermi momentum and the mass of the charge carriers, and c is the speed of light. Therefore, it is of general interest to propose 1D plasma models allowing both degeneracy and relativistic features. Specifically, in this work we investigate the relativistic fluid dynamics of ion-acoustic structures in electrostatic plasmas, where the electron-degeneracy is described by an equation of state similar to that of Chandrasekhar [16]. On the other hand, we consider a cold non-degenerate ion fluid, without the inclusion of a Fermi pressure, due to their larger mass. We have to emphasize that there are many models in the literature dealing in a non-rigorous way with relativistic effects on quantum ion-acoustic waves in dense plasmas. See more comments on this regard in the next Section.

Our aim here is to propose a relativistic fluid model for ion-acoustic excitations in 1D plasmas taking into account the electron degeneracy. The layout of this work goes as follows. First, the basic equations are presented and manipulated algebraically for convenience. This is followed by a brief discussion on the choice of scaling, leading to a dimensionless set of model equations, to form the basis of our analysis. A linear treatment leads to a dispersion relation for small-amplitude ion-acoustic waves. We then proceed by adopting the Sagdeev pseudopotential method for stationary-profile excitations. Plots of numerical solutions, in the form of pulse-shaped solitary waves, are presented, and their existence region and dynamical properties are investigated. Finally, our conclusions are outlined in the concluding section.

II. HYDRODYNAMIC MODEL

The model comprises the particle number (mass) and momentum conservation equations for the two separate electron and ion fluids, with the system closed by Poisson's equation:

$$\begin{aligned}
&\frac{\partial \gamma_i n_i}{\partial t} + \frac{\partial}{\partial x}(\gamma_i n_i v_i) = 0\,,\\
&\frac{\partial \gamma_e n_e}{\partial t} + \frac{\partial}{\partial x}(\gamma_e n_e v_e) = 0\,,\\
&\left(\frac{\partial}{\partial t} + v_i \frac{\partial}{\partial x}\right)\gamma_i v_i + \frac{e}{m_i}\frac{\partial \phi}{\partial x} = 0\,,\\
&\\
&m_e H \left(\frac{\partial}{\partial t} + v_e \frac{\partial}{\partial x}\right)\gamma_e v_e =\\
&-\frac{\gamma_e}{n_e}\left(\frac{\partial}{\partial x} + \frac{v_e}{c^2}\frac{\partial}{\partial t}\right) P_e + e\frac{\partial \phi}{\partial x}\,,\\
&\frac{\partial^2 \phi}{\partial x^2} + \frac{e}{\epsilon_0}(\gamma_i n_i - \gamma_e n_e) = 0\,. \qquad (1)
\end{aligned}$$

The equations are obtained from the equations for a neutral isotropic ideal fluid at rest by means of Lorentz transformation [17]. In the case of charged fluids, one considers the virtual variations of the electromagnetic stress-energy tensor; see [18, 19] for details. Furthermore, $m_{e,i}$ is the rest mass of the electrons (respectively ions); $v_{e,i}$ is the velocity of the electrons (respectively ions); $\gamma_{e,i} = (1 - v_{e,i}^2/c^2)^{-1/2}$ is the relativistic dilation factor for electrons (respectively ions); ϕ is the electrostatic potential; P_e is the pressure of the electrons; e is the fundamental unit of electric charge; h is Planck's constant and ϵ_0 is the permittivity of vacuum.

In our work we adopt a general equation of state for a fully-degenerate fermion gas in one dimension, which is valid for all values of the relativistic parameter, $p_F/m_e c$, where p_F is the electrons Fermi momentum. In contrast, e.g. Ref. [19] employs a 3D polytropic equation of state $P_e \sim n_e^\alpha$, see Eq. (13) therein, focusing specifically on the particular values $\alpha = 5/3$ and $\alpha = 4/3$, which correspond respectively to the non-relativistic and ultra-relativistic limits for a fully-degenerate fermion gas in three dimensions. For the sake of comparison, the non-relativistic and ultra-relativistic cases in our 1D model would give respectively $P_e \sim n_e^3$ and $P_e \sim n_e^2$. The Fermi pressure, P_e, is given by

$$P_e = \frac{2m_e^2 c^3}{h}\left(\xi(\xi^2+1)^{1/2} - \sinh^{-1}(\xi)\right)\,, \qquad (2)$$

and the related non-dimensional enthalpy density (pressure plus internal mass-energy density), H, is defined as

$$H = \sqrt{1+\xi^2}\,, \qquad (3)$$

where

$$\xi = \frac{h n_e}{4 m_e c}. \qquad (4)$$

The function H is related to relativistic mass increase due to thermal (not bulk) motion.

Equation (2) applies for a fully degenerate ideal 1D electron gas admitting relativistic effects and is reminiscent of the Chandrasekhar 3D equation of state used to describe equilibria in dense stars [16]. It has been derived by Chavanis in the discussion of white dwarf equilibria in arbitrary dimensionality [20]. It also appears in the analysis of wave-breaking amplitude of relativistic oscillations in a thermal plasma described by a water bag equilibrium [21], in this case without connection to Fermi-Dirac statistics.

The non-relativistic equation of state $P_e = p_F^2 n^3/(3m_e n_0^2)$ is recovered by expanding around $\xi = 0$, which formally corresponds to $c \to \infty$ in the non-relativistic approximation. Here the subscript 0 denotes the value at equilibrium and $p_F = h n_0/4$ is the 1D expression of the Fermi momentum. In this context, the present work is a relativistic complement to the fluid theory of quantum ion-acoustic waves in 1D geometry [22]. However, presently we do not include quantum diffraction effects, which would manifest through a Bohm potential term. Typically, for very large densities, quantum effects arising from the Fermi-Dirac statistics (Pauli's exclusion principle) are dominant in comparison to the quantum contributions coming from the wave nature of the charge carriers. However, quantum diffraction is essential at nanoscales, for instance in the treatment of ultra-small electronic devices [23].

The conditions for considering a degenerate electron fluid and a cold non-degenerate ion fluid can be summarized via the following ordering:

$$T_{Fi} \ll T_i \ll T_e \ll T_{Fe}\,, \qquad (5)$$

where $T_{Fe,Fi}$ denote the electrons (ions, respectively) Fermi temperature and $T_{e,i}$ are the electrons (ions) thermodynamic temperatures, respectively. However, unlike in Ref. [22], here we do not impose that the electrons' Fermi energy should be much smaller than the electrons rest energy. Moreover, general relativity and/or QED effects are not included in our treatment, since for instance we limit ourselves to electric field amplitudes smaller than Schwinger's field strength $E_S = m_e^2 c^3/e\hbar \simeq 10^{18} V/m$. In the same footing, the involved plasmon energies will be assumed to be much smaller than $2m_e c^2$, so that pair creation processes are disregarded (this is reasonable except for extremely small wavelengths). In addition, a fluid treatment is adequate as long as kinetic effects such as Landau damping are not decisive. Note that in 1D geometry a fully degenerate electrons particle distribution function is flat, so that there is no collisionless damping. Finally, the theory is restricted to weakly-coupled plasmas.

It is instructive to discuss in more detail the full degeneracy assumption

$$E_{Fe} = \sqrt{p_F^2 c^2 + m_e^2 c^4} - m_e c^2 \gg \kappa_B T_e\,, \qquad (6)$$

where κ_B is Boltzmann's constant.

This involves the understanding of the 1D equilibrium number density n_0, which can be viewed in correspondence to a 3D equilibrium number density n_{3D} according to

$$n_0 = \frac{1}{2r_s} = \left(\frac{\pi n_{3D}}{6}\right)^{1/3}, \tag{7}$$

where r_s is the Wigner-Seitz radius. In this context we are considering adjacent spherical "particles" occupying a sphere of radius r_s, with a mean inter-particle separation $2r_s$. For instance, in the case of white dwarfs one has $n_{3D} = 10^{36}m^{-3}$ and $n_0 = 8.0 \times 10^{11}m^{-1}$. Taking into account the 1D expression of the Fermi momentum, it is found that electrons would be fully degenerate provided $T_e \ll 6.7 \times 10^8 K$.

The model is recast in dimensionless form by the following scaling,

$$\begin{aligned} t \mapsto \omega_{pi} t\,, \qquad & x \mapsto \omega_{pi} x/c_s\,, \\ n_{e,i} \mapsto n_{e,i}/n_0\,, \qquad & v_{e,i} \mapsto v_{e,i}/c_s\,, \qquad \phi \mapsto e\phi/2\tilde{E}_{Fe}\,, \end{aligned} \tag{8}$$

where $\omega_{pi} = \sqrt{e^2 n_0/\epsilon_0 m_i}$ is the ion plasma frequency, $c_s = \sqrt{2\tilde{E}_{Fe}/m_i} = hn_0/4\sqrt{m_i m_e}$ is the non-relativistic ion-acoustic speed in terms of the non-relativistic electrons Fermi energy $\tilde{E}_{Fe} = p_F^2/2m_e$ and n_0 is the equilibrium density, which is the same for both electrons and ions by Poisson's equation. After a little algebra, the dimensionless model is expressed as

$$\begin{aligned} &\frac{\partial \gamma_i n_i}{\partial t} + \frac{\partial}{\partial x}(\gamma_i n_i v_i) = 0\,, \\ &\frac{\partial \gamma_e n_e}{\partial t} + \frac{\partial}{\partial x}(\gamma_e n_e v_e) = 0\,, \\ &\frac{\partial \gamma_i v_i}{\partial t} + v_i \frac{\partial \gamma_i v_i}{\partial x} + \frac{\partial \phi}{\partial x} = 0\,, \\ &\frac{m_e}{m_i} H \left(\frac{\partial \gamma_e v_e}{\partial t} + v_e \frac{\partial \gamma_e v_e}{\partial x}\right) = \\ &-\frac{n_e \gamma_e}{H}\left(\frac{\partial n_e}{\partial x} + \alpha v_e \frac{\partial n_e}{\partial t}\right) + \frac{\partial \phi}{\partial x}\,, \\ &\frac{\partial^2 \phi}{\partial x^2} + \gamma_i n_i - \gamma_e n_e = 0\,, \end{aligned} \tag{9}$$

in terms of the parameters

$$\xi_0 = \frac{p_F}{m_e c}\,, \quad \alpha = \frac{c_s^2}{c^2} = \frac{m_e}{m_i}\xi_0^2\,. \tag{10}$$

It is apparent that the relativistic parameter ξ_0 is the only remaining numerical constant in the model. The non-relativistic limit is simply $\xi_0 \ll 1$.

Finally, in terms of the rescaled variables, we have the relativistic factor $\gamma_{e,i} = (1 - \alpha v_{e,i}^2)^{-1/2}$.

In passing, we note that even if the parameter α is small (e.g. due to $\xi_0 < 1$ and also $m_e/m_i \ll 1$), in case of strong nonlinearities the terms containing α may in principle be important. In particular, there is no *a priori* methodological reason to quickly discard the time-derivative of the pressure, manifesting in the $\propto \partial n_e/\partial t$ contribution in the electrons force equation in Eq. (9). Note also that we do not discard the electrons' convective derivative, because after restoring physical coordinates it can be shown that the Fermi pressure vanishes in the inertialess limit (formally $m_e/m_i \to 0$). Moreover the inclusion of the electrons' convective derivative ultimately leads to a considerable simplification.

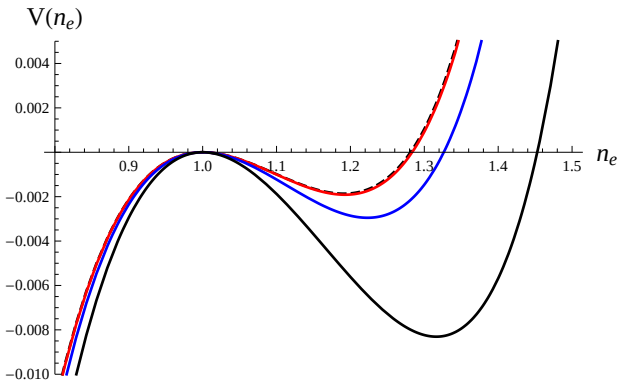

FIG. 1: (Color online) Plots of the pseudopotential, $V(n_e)$, for different values of equilibrium density, n_0. The curves crossing the n_e-axis at $n_e = 1.45$ (black, bottom), $n_e = 1.33$ (blue, mid) and $n_e = 1.28$ (red, upper) correspond to $n_0 = 10^{12}m^{-1}$, $n_0 = 5 \times 10^{11}m^{-1}$ and $n_0 = 10^{11}m^{-1}$ respectively. The Mach number is $M = 1.2$. The dashed curve represents the non-relativistic pseudopotential and is a good approximation to $V(n_e)$ for lower equilibrium densities.

III. LINEAR APPROXIMATION

Let us begin our analysis by considering the small-amplitude limit of the above system of equations (9).

We consider plane waves of the form

$$\begin{aligned} n_{e,i} &= 1 + n_{e,i1} e^{i(kx-\omega t)} + \bar{n}_{e,i1} e^{-i(kx-\omega t)}\,, \\ v_{e,i} &= v_{e,i1} e^{i(kx-\omega t)} + \bar{v}_{e,i1} e^{-i(kx-\omega t)}\,, \\ \phi &= \phi_1 e^{i(kx-\omega t)} + \bar{\phi}_1 e^{-i(kx-\omega t)}\,, \end{aligned} \tag{11}$$

where the bar denotes complex conjugation and where quantities with a subscript "1" are of the same order of magnitude, which is much less than unity. Linearizing and retaining only first-order harmonics, we obtain the following set of linear algebraic equations:

$$\begin{aligned} &-\omega n_{i1} + k v_{i1} = 0\,, \\ &-\omega n_{e1} + k v_{e1} = 0\,, \\ &-\omega v_{i1} + k\phi_1 = 0\,, \\ &-\frac{m_e}{m_i}\omega v_{e1}\sqrt{1+\xi_0^2} - k\phi_1 + \frac{n_{e1}}{\sqrt{1+\xi_0^2}}k = 0\,, \\ &-k^2\phi_1 + n_{i1} - n_{e1} = 0\,. \end{aligned} \tag{12}$$

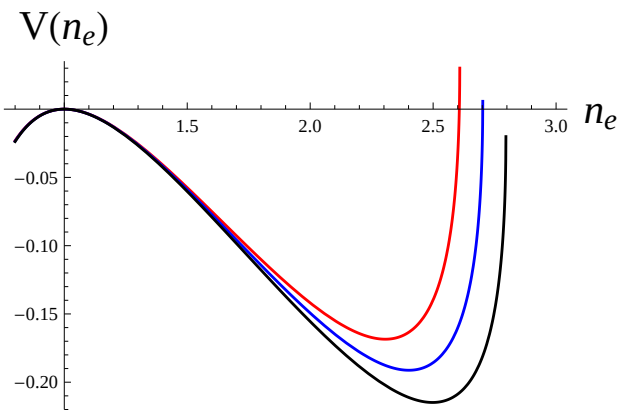

FIG. 2: (Color online) Plots of the pseudopotential, $V(n_e)$, for three values of M. $n_0 = 10^{11} m^{-1}$ throughout. The curve for $M = 2.6$ (black, bottom) does not cross the n_e-axis and so does not admit soliton solutions. The curve for $M = 2.5$ (blue, mid) crosses the axis at $n_e = 2.6$ and the remaining curve (red, upper) represents $M = 2.4$.

These equations can be rearranged to yield a dispersion relation for the angular frequency ω in terms of the wavenumber k. As in classical plasma, this relation consists of two branches: a low-frequency modified ion-acoustic mode, and a higher frequency (electron plasma) optical-like mode. These will be discussed elsewhere in detail. Since we focus on the ionic dynamical scale here, of interest to us is the former (acoustic) mode, which can be approximated for small k as follows:

$$\omega^2 \approx \frac{k^2}{\delta + k^2}, \tag{13}$$

where we have defined the constant:

$$\delta = \left(1 + \frac{m_e}{m_i}\sqrt{1+\xi_0^2}\right)\sqrt{1+\xi_0^2}\,. \tag{14}$$

There is also a high frequency (Langmuir) mode, which we do not consider any further in this work.

The phase speed in the long wavelength (small wavenumber, $k \ll 1$) limit is obtained as

$$v_{ph} = \frac{\omega}{k} \simeq \frac{1}{\sqrt{\delta}}\,. \tag{15}$$

We draw the conclusion that the quantity δ defined above contains the essential physics of the (linear) problem; in fact, its square root is directly related to the (inverse) screening length, and is also proportional to the "true" acoustic speed (phase speed) in our plasma configuration.

IV. TRAVELLING-WAVE ANALYSIS

Anticipating stationary profile solutions, we start with the assumption that n_j, v_j and ϕ are all functions of a single variable, $X = x - Mt$. Here the (scaled) pulse speed M is the so-called "Mach" number, i.e. the ratio of the actual pulse speed to the ion sound speed. At this point M is a real parameter which is left arbitrary. Its range of values will be investigated later. The model can thus be rewritten as

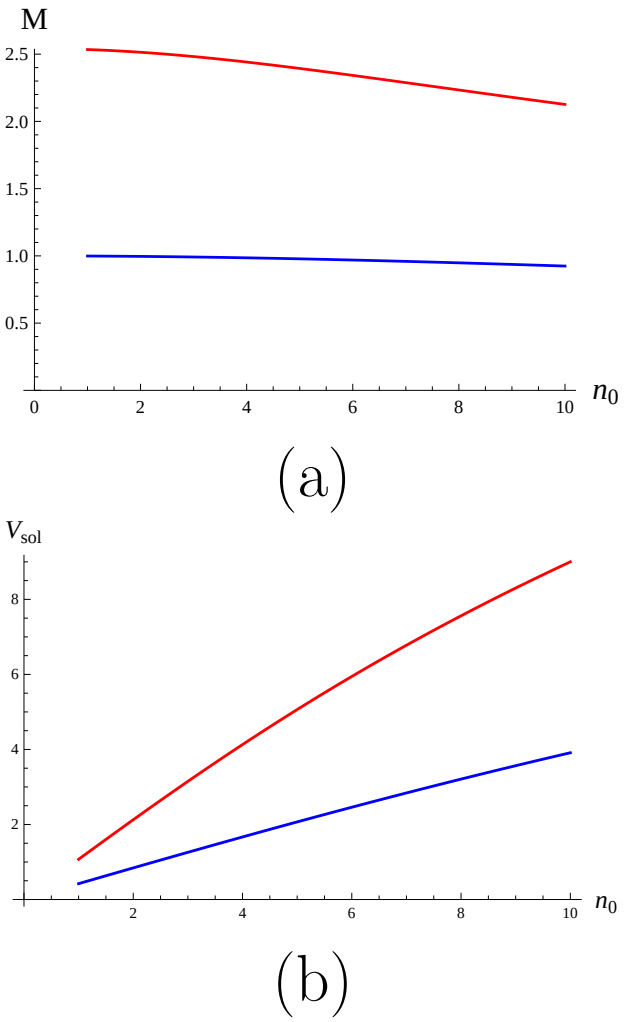

FIG. 3: (Color online) The domain of existence is within the two lines: upper Mach number (red, upper) and lower Mach number (blue, bottom). Density is given in units of $10^{11} m^{-1}$. (a) shows M in dimensionless form and (b) shows the corresponding true speed, V_{Sol}, in units of $10^6 m s^{-1}$ once dimensions have been restored.

$$-M\,(\gamma_i n_i)' + (\gamma_i n_i v_i)' = 0\,, \tag{16}$$

$$-M\,(\gamma_e n_e)' + (\gamma_e n_e v_e)' = 0\,, \tag{17}$$

$$-M\,(\gamma_i v_i)' + v_i\,(\gamma_i v_i)' + \phi' = 0\,, \tag{18}$$

$$\frac{\gamma_e n_e}{H}(1 - \alpha M v_e) n_e' - m_e H (M - v_e)(\gamma_e v_e)' = \phi'\,, \tag{19}$$

$$\phi'' = \gamma_e n_e - \gamma_i n_i\,, \tag{20}$$

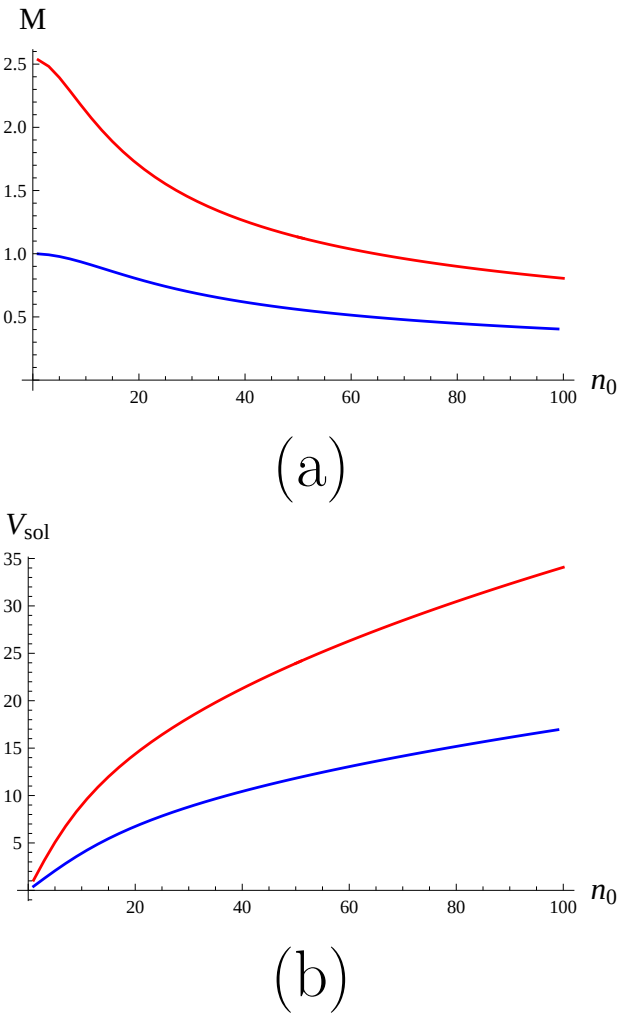

FIG. 4: (Color online) Extending Fig.3 to a large range of of equilibrium density suggests that there is no intersection between the upper and lower Mach numbers and, therefore, that solitons can exist as solutions to this model for any non-zero value of n_0. Density is given in units of $10^{11}m^{-1}$. V_{Sol} is given in units of $10^6 ms^{-1}$ in (b). Upper Mach number: red, upper; lower Mach number: blue, bottom.

where primes denote differentiation with respect to X. We adopt appropriate boundary conditions:

$$\lim_{X\to\pm\infty} n_{e,i} = 1; \quad \lim_{X\to\pm\infty} v_{e,i} = 0; \quad \lim_{X\to\pm\infty} \phi = 0. \tag{21}$$

Integrating (16)-(18) over the interval $(-\infty, X]$, three useful relations are recovered:

$$n_{i,e} = \frac{M}{\gamma_{i,e}(M - v_{i,e})}, \tag{22}$$

$$\phi = M\gamma_i v_i - \frac{\gamma_i}{\alpha} + \frac{1}{\alpha}. \tag{23}$$

The above relation can be inverted to find v_i in terms of ϕ,

$$v_i = \frac{\frac{M}{\alpha} - \sqrt{\frac{M^2}{\alpha^2} - \left[M^2 + \alpha(\frac{1}{\alpha} - \phi)^2\right]\left[\frac{1}{\alpha^2} - (\frac{1}{\alpha} - \phi)^2\right]}}{M^2 + \alpha\left(\frac{1}{\alpha} - \phi\right)^2}, \tag{24}$$

where the negative sign has been adopted in the numerator in order to agree with boundary conditions.

Equation (19) can be manipulated to yield an expression for ϕ in terms of n_e:

$$\phi(n_e) = \frac{1}{\xi_0^2}\left(\gamma\sqrt{1 + \xi_0^2 n^2}\,(1 - \alpha M v_e) - \sqrt{1 + \xi_0^2}\right). \tag{25}$$

It is here that the advantage of retaining the electrons' convective derivative manifests itself: writing $v(\gamma v)'$ as γ'/α allows this convective term to be expressed in such a manner as to cancel the pressure term. To ignore the convective term leads to an expression for the electric potential containing elliptic integrals, which is decidedly less compact and is unnecessarily complicated as a description.

Poisson's relation is manipulated to obtain the following integral.

$$\begin{aligned}
\frac{1}{2}\phi'^2 &= \int_{-\infty}^{X} d\tilde{X}\phi'(\gamma_e n_e - \gamma_i n_i) \\
&= \int_{-\infty}^{X} d\tilde{X}\phi'\gamma_e n_e - \int_{-\infty}^{X} d\tilde{X} v_i' f(v_i)\gamma_i n_i \\
&= \int_{-\infty}^{X} d\tilde{X}\phi'\gamma_e n_e - \int_{0}^{v_i} dv f(v)\gamma n \\
&= I_e - I_i.
\end{aligned} \tag{26}$$

In the latter relation, I_e and I_i denote respectively the first and second integrals in the right-hand side and

$$f(v) = (M - v)\,\gamma^3\,. \tag{27}$$

We arrive at a pseudo-balance equation with $S(\phi) = I_i - I_e$:

$$\frac{1}{2}\left(\frac{d\phi}{dX}\right)^2 + S(\phi) = 0. \tag{28}$$

The "pseudopotential" function, $S(\phi)$, determines the behavior of the solution to the above differential equation through the properties of its roots (whether they exist, whether they are also stationary points and, if so, the nature of these stationary points). The pseudopotential methodology is well-known (though mostly in classical system) [24], and the algebraic toolbox accompanying it has evolved, since its first appearance; details can be found e.g. in Ref. 25.

The ions' contribution to the pseudopotential is straightforward to evaluate:

$$I_i = \int_0^{v_i} dv_i M\gamma_i^3 = Mv_i\gamma_i\,. \tag{29}$$

An expression for I_e is obtained after integrating by parts. The derived relation is given in terms of n_e as a matter of convenience because, although the function $\phi(n_e)$ (25) is easily inverted to find n_e in terms of ϕ, it is much easier to work with the electron density.

$$S(n_e) = \left[M\gamma_i v_i - \gamma n\left(\phi(n) + \frac{\sqrt{1+\xi_0^2}}{\xi_0^2}\right) + \frac{1}{2\xi_0^3}\left(\sinh^{-1}(\xi_0 n) + \xi_0 n\sqrt{1+\xi_0^2 n^2}\right)\right]_{n=1}^{n=n_e} \tag{30}$$

where $[f(n)]_{n=a}^{n=b} = f(b) - f(a)$. In order to write (28) in terms of n_e, we make use of (24) and (22) in conjunction with $\phi(n_e)$ to obtain v_e, v_i and n_i as functions of n_e. Finally, the chain rule for differentiation is used to yield the pseudo-balance equation:

$$\frac{1}{2}\left(\frac{dn_e}{dX}\right)^2 + V(n_e) = 0, \tag{31}$$

where the new pseudopotential form, $V(n_e)$, is given by:

$$V(n_e) = \left(\frac{d\phi}{dn_e}\right)^{-2} S(\phi)\,. \tag{32}$$

There is considerable difference between this relativistic pseudopotential and its non-relativistic equivalent ($V_{NR}(n_e)$, given below). This pseudopotential is given in terms of the same scaling as relativistic counterpart. Note that the equilibrium density, n_0, plays no part in the dynamics. In contrast, the relativistic case contains an extra dependence on n_0 by way of $\xi_0 (= p_{Fe0}/m_e c)$. Note that v_i in $V_{NR}(n_e)$ refers to the non-relativistic ion fluid speed. In Fig. 1, it is shown that the non-relativistic case is a good approximation to $V(n_e)$ for low densities in the specific case shown ($M = 1.2$). This is true in general for different Mach numbers. Indeed, it is a straightforward task to show by means of a Maclaurin series expansion that $V_{NR}(n_e)$ is an approximation to third order in n_e for $\xi_0 \approx 0$.

$$V_{NR}(n_e) = \frac{1}{n_e^2}\left(Mv_i - \frac{1}{3}(n_e^3 - 1)\right). \tag{33}$$

V. EXISTENCE CONDITIONS

A series of algebraic constraints should be imposed on the value of the (real) parameter M, in fact representing physical constraints on the value of the pulse speed [24, 25].

A. Acoustic limit – lower M boundary.

For this section, it will be easier to work with $S(\phi)$ instead of $V(n_e)$. A double root is assumed to exist at equilibrium (where $n_e = 1$, $v_{e,i} = 0$ and $\phi = 0$), recovered for $X \to \pm\infty$, so that the system may depart from equilibrium and generate the described excitation. The following should hold as an identity:

$$\begin{aligned} S(\phi) &= \int_0^{\phi} d\tilde{\phi} \quad \gamma_i n_i(\tilde{\phi}) - \gamma_e n_e(\tilde{\phi}) \\ \Rightarrow \frac{dS(\phi)}{d\phi} &= \gamma_i n_i - \gamma_e n_e \quad (= 0 \text{ when } \phi = 0)\,. \end{aligned} \tag{34}$$

The nature of this double root depends on the specific model and is dependent on the value of M. The calculation shown below results from a manipulation of the integrated equations of continuity and from (23).

From (22), we have

$$\gamma_{e,i} n_{e,i} = \frac{M}{M - v_{e,i}},$$

which leads to

$$v_{e,i} = \frac{Mn_{e,i}^2 - \sqrt{\alpha M^4 + n_{e,i}^2(M^2 - \alpha M^4)}}{n_{e,i}^2 + \alpha M^2} \tag{35}$$

and, accordingly,

$$\begin{aligned} \gamma_{e,i} n_{e,i} &= \frac{n_{e,i}^2 + \alpha M^2}{\alpha M^2 + \sqrt{\alpha M^2 + n_{e,i}^2(1 - \alpha M^2)}} \\ &= \frac{\sqrt{\alpha M^2 + n_{e,i}^2(1 - \alpha M^2)} - \alpha M^2}{1 - \alpha M^2}. \end{aligned} \tag{36}$$

(For brevity, we have proceeded with both subscripts 'e' and 'i' for electrons and ions, respectively.) Then,

$$\begin{aligned} \frac{d\gamma_{e,i} n_{e,i}}{dn_{e,i}} &= \frac{n_{e,i}}{\sqrt{\alpha M^2 + n_{e,i}^2(1 - \alpha M^2)}} \\ &\left(= 1 \qquad \text{at } n_{e,i} = 1\right). \end{aligned} \tag{37}$$

Therefore,

$$\begin{aligned} \frac{d^2 S(\phi)}{d\phi^2} &= \frac{dn_i}{d\phi}\frac{d\gamma_i n_i}{dn_i} - \frac{dn_e}{d\phi}\frac{d\gamma_e n_e}{dn_e} \\ &\left(= \frac{dn_i}{d\phi} - \frac{dn_e}{d\phi} \qquad \text{at } n_{e,i}{=}1\right). \end{aligned} \tag{38}$$

For the density variables, we have

$$\frac{dn_e}{d\phi} = \frac{m_i\sqrt{1+\xi_0^2}}{m_i - m_e M^2(1+\xi_0^2)} \qquad (\text{at } n_e = 1)\,, \tag{39}$$

and

$$\begin{aligned}\frac{dn_i}{dv_i} &= \frac{d}{dv_i}\frac{M}{\gamma_i(M-v_i)} \\ &= -\alpha v_i\gamma_i\frac{M}{M-v_i} + \frac{1}{\gamma_i}\frac{M}{(v_i-M)^2} \\ \left(\right. &= \frac{1}{M} \qquad \text{at } n_i = 1)\,. \end{aligned} \tag{40}$$

Finally, the ion velocity in the moving frame is given by:

$$\frac{dv_i}{d\phi} = \frac{1}{\gamma_i^3(M-v_i)} \qquad \left(\right. = \frac{1}{M} \qquad \text{at } n_i = 1)\,. \tag{41}$$

Combining the last relations gives, at $\phi = 0$,

$$\frac{d^2S(\phi)}{d\phi^2} = \frac{1}{M^2} - \frac{\sqrt{1+\xi_0^2}}{1 - m_e M^2(1+\xi_0^2)/m_i}\,, \tag{42}$$

which is negative (condition imposed for a local maximum) for

$$M > \frac{1/(1+\xi_0^2)^{1/4}}{(1+m_e(1+\xi_0^2)^{1/2}/m_i)^{1/2}} = 1/\delta^{1/2} \equiv M_1. \tag{43}$$

The threshold M_1 thus obtained is precisely equal to the true "sound" (acoustic) speed in the given plasma configuration, as obtained by a linear treatment (refer to (15) in Sec. III). We deduce that the pulse speed M must be greater than the phase speed of linear waves. This formula can be approximated by $M_1 \approx 1 - \xi_0^2/4$ for $\xi_0 \approx 0$ and by $M_1 \approx 1/\sqrt{\xi_0}$ for $\xi_0 \gg 1$.

B. Reality condition – upper Mach number limit.

A second condition on M arises from reality considerations. Recalling that the ion speed v_i is given in terms of the electric potential ϕ by expression (24), we note that reality of the ion speed variable imposes that the argument of the square root in (24) must be non-negative. A maximum value of ϕ is that imposed, viz.

$$\phi < \frac{1}{\alpha}\left(1 - \sqrt{1-\alpha M^2}\right) = \phi_{max}\,. \tag{44}$$

Clearly, the non-relativistic case ($\phi_{max} = M^2/2$) is recovered in the non-relativistic limit ($\alpha \ll 1$). Indeed, this can be written in a manner more illuminating:

$$\phi_{max} = \frac{(\gamma(M)-1)}{\alpha\gamma(M)}, \tag{45}$$

where $\gamma(x) = (1-\alpha x^2)^{-1/2}$. The numerator has the form of relativistic kinetic energy. Upon restoration of dimensions, we find for the real potential (denoted here only as $\Phi = \phi m_i c_s^2$)

$$e\Phi = \frac{m_i c^2(\gamma(M)-1)}{\gamma(M)}. \tag{46}$$

The equivalent expression in the non-relativistic case, which can be obtained directly from the non-relativistic model or by a Maclaurin expansion of the above, is known to be

$$e\Phi_{max} = \frac{m_i}{2}M^2c_s^2 = \frac{m_i}{2}V_{sol}^2\,. \tag{47}$$

Once again, note that the density plays a stronger role in the relativistic expression. The extra contributions beyond what is absorbed in the scaling "drop out" in the non-relativistic limit.

We emphasize that (44) is not necessarily the least upper bound for a given plasma configuration, i.e. other constraints may be violated before the upper bound is attained.

Provided $S(\phi)$ is negative between its two roots, there can exist bound solutions. It has been shown that there is necessarily a root at $\phi = 0$. The second root corresponds to the maximum value of ϕ for the configuration (M, n_0) of the system. For M less than a certain maximum, the potential crosses the n_e-axis before it becomes complex (where violation of $\phi < \phi_{max}$ occurs). See Fig. 2 for a graphical illustration of this.

Reverting to the pseudopotential $V(n_e)$, if it becomes complex before it reaches its second root, then there can be no real, bound solutions. Therefore, the maximum value, M_2, of M occurs where the second root coincides with $n_{e,max}$, which is obtained from ϕ_{max} given in (44). In other words, the upper bound, M_2, is obtained numerically by solving $V(n_e = n_{e,max}) = 0$ – viz. $S(\phi = \phi_{max}) = 0$ (the lengthy expression is omitted here).

The lower and upper Mach numbers for a range of values of the equilibrium density are depicted in Fig. 3, both in their dimensional and dimensionless form. Recall that pulse excitations exist between the two curves.

VI. PARAMETRIC ANALYSIS

The closed-form expression for the pseudopotential, $V(n_e)$ (30), allows us to quickly identify general trends, provided we bear in mind that a change in equilibrium density will change the scales accordingly. The domain of existence of our solution for fixed equilibrium density is defined in the lower limit by the maximum phase speed and in the upper limit by the value of M at which $V(n_{max}) = 0$ (equivalently $S(\phi_{max}) = 0$) (c.f. Sec. V). A graphical illustration of this point can be seen in Fig.

2, wherein the curve corresponding to $M = 2.4$ will admit localized solutions whereas the curve for $M = 2.6$ will not. A plot of the existence region for a range of values of n_0 is given in Fig. 3. It should be noted that, although this plot appears to show a decreasing trend in the upper limit, M is measured in units of c_s, which increases linearly with n_0. The second plot in Fig.3 shows the true speeds corresponding to these Mach numbers, which we label V_{Sol}. The range of densities considered here correspond to a 3D density of around $10^{36}m^{-3}$, or that of a white dwarf star.

Fig. 4 reproduces the same type of plot(s) for a wider range of densities, here provided for the sake of comparison. This is provided for illustrative purposes, as the corresponding densities are too high for today's high-density plasma systems of interest.

The pseudoenergy balance equation (31) is integrated numerically to find n_e as a function of X, M and n_0. This can then be used to plot ϕ, v_e, v_i, n_i and the electric field, $E = -d\phi/dX$. Fig. 5 gives these functions for different values of M. For all, an increase in M results in an increase in the respective scaled quantity in scaled units. Fig. 6 shows the complementary arrangement, with M being fixed and n_0 differing between the curves.

As Fig. 2 suggests, the maximum value of n_e, here labeled n_m, for a fixed equilibrium density increases as M increases. (Recall that n_m is not necessarily the same as $n_{max} = n(\phi = \phi_{max})$, where ϕ_{max} was given in (44).) This is depicted in Fig. 7(a), where the trend is shown for three values of n_0.

The same trend is exhibited by the maximum value, ϕ_m, of the electrostatic potential; see Fig. 7(b). It must be emphasized that these plots are dimensionless. However, since n_m is scaled by n_0 and M by $hn_0/4\sqrt{m_i m_e}$ (recall the definition in Sec. II), the general trends in n_m for different M and n_0 are qualitatively unchanged upon restoration of dimensions.

On the other hand, ϕ_m in Fig. 7(b) is scaled by n_0^2, so the gradients would be multiplied by a factor proportional to n_0 if dimensions were restored. However, the qualitative trend of the curves would not change in this case.

VII. CONCLUSIONS

We have examined the dynamical characteristics (conditions for occurrence, structural features) of large amplitude nonlinear pulse-shaped structures in degenerate plasmas, by making use of a self-consistent relativistic formalism. We have assumed cold relativistic ions. The equation of state for an ideal fully-degenerate, relativistic electron gas in 1D has been applied.

In the non-relativistic limit, the standard equation of state for ideal fully-degenerate plasma is recovered.

The model has been shown to admit localized solutions within certain constraints on the density of the plasma and on the ion-fluid speed. A pseudobalance equation was derived in a closed form and was then integrated numerically to plot such solutions for a wide range of densities and speeds.

We find that the amplitude of our solutions increases with M for fixed density. A similar increase is observed by holding M fixed and increasing the density, which corresponds to a "more relativistic" system.

Our results address for the first time the physical setting of nonlinear structures in degenerate plasmas, adopting a rigorous, strictly one-dimensional relativistic formulation. Our findings are of relevance in physical settings where ultradense material configurations occur [2–8].

Acknowledgments

The authors acknowledge support from the EU-FP7 IRSES Programme (grant 612506 QUANTUM PLASMAS FP7-PEOPLE-2013-IRSES). FH and IK gratefully acknowledge support from the Brazilian research fund CNPq (Conselho Nacional de Desenvolvimento Científico e Tecnológico - Brasil).

[1] T. Giamarchi, *Quantum Physics in One Dimension* (Oxford University Press, New York, 2004).
[2] M. Passoni, L. Bertagna and A. Zani A., *New J. Phys.* **12**, 0450122 (2010).
[3] R. Thiele, P. Sperling, M. Chen *et al., Phys. Rev. E* **82**, 056404 (2010).
[4] P. K. Shukla and B. Eliasson, *Phys. Rev. Lett.* **100**, 036801 (2008).
[5] G. Barak, H. Steinberg, L. N. Pfeiffer *et al.*, *Nature Physics* **6**, 489 (2010).
[6] A. Imambekov and L. I. Glazman, *Science* **323**, 228 (2009).
[7] F. Haas, G. Manfredi, P. K. Shukla and P.-A. Hervieux, *Phys. Rev. B* **80**, 073301 (2009).
[8] S. Ghosh, N. Chakrabarti and F. Haas, *Europhys. Lett.* **105**, 30006 (2014).
[9] M. McKerr, I. Kourakis and F. Haas, *Plasma Phys. Controll. Fusion* **56**, 035007 (2014).
[10] M. Akbari-Moghanjoughi, *Astrophys. Space Sci.* **332**, 187 (2011).
[11] A. Rahman and S. Ali, *Astrophys. Space Sci.* **351**, 165(2014).
[12] V. Canuto and J. Ventura, *Astrophys. Space Sci.* **18**, 104 (1972).
[13] V. Canuto and J. Ventura, Fundamentals of Cosmic Physics, Vol. 2 (Gordon and Breach Science Publishers, UK, 1977).
[14] P. Carbonaro, *Il Nuovo Cimento* **103**, 485 (1989).
[15] E. E. Salpeter, *Astrophys. J.* **134**, 669 (1961).
[16] S. Chandrasekhar, *Mon. Not. R. Astron. Soc.* **95**, 207

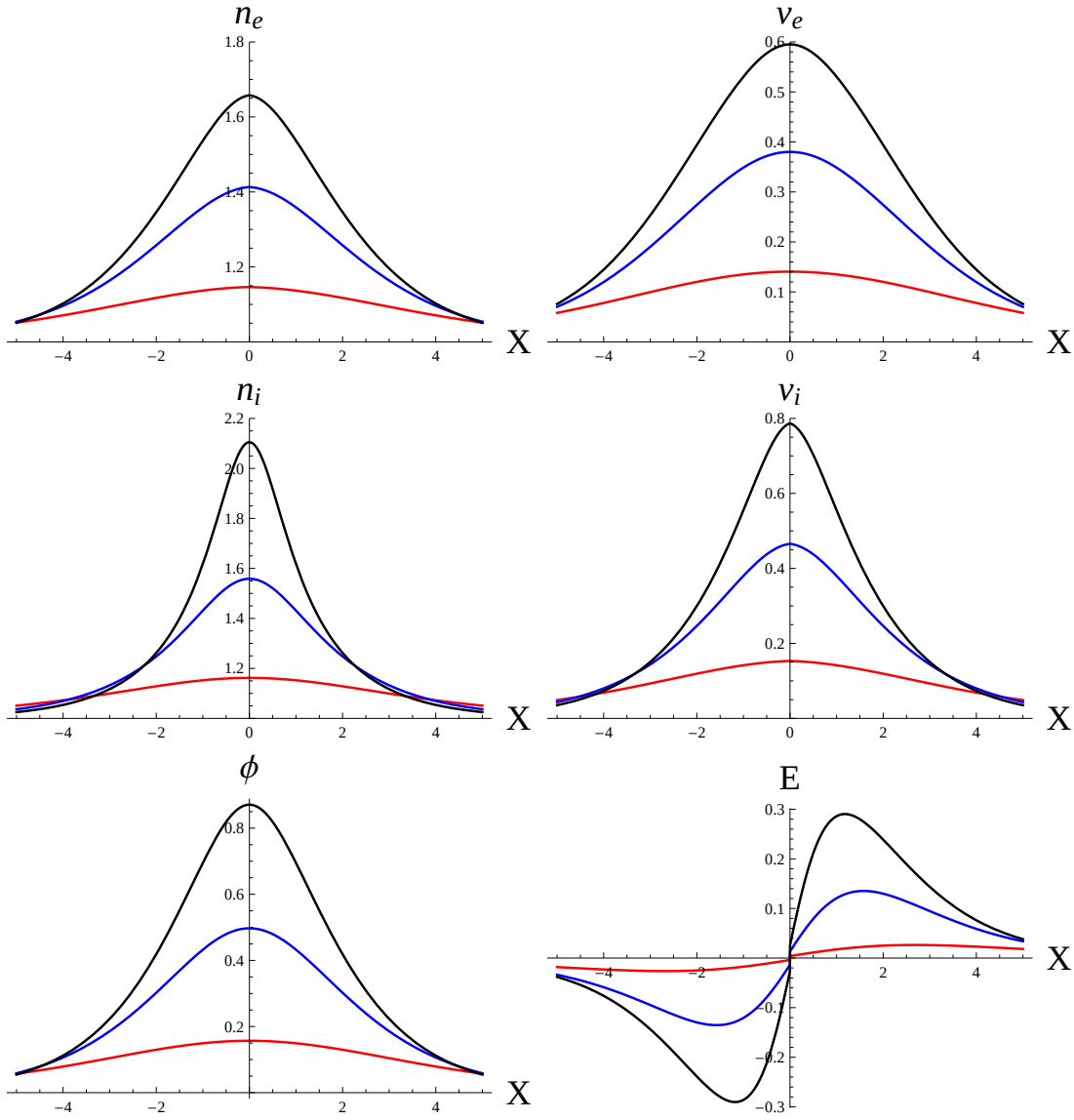

FIG. 5: (Color online) Plots of the plasma state variables are given, for different values of the Mach number. Here, $n_0 = 10^{11} m^{-1}$ throughout. With reference to the right-hand side of each graph, the upper (black), middle (blue) and lower (red) curves correspond to $M = 1.5$, 1.3 and 1.1 respectively.

(1935).
[17] S. Weinberg, Gravitation and Cosmology, (John Wiley and Sons, New York, 1972).
[18] V. I. Berezhiani and S. M. Mahajan, *Phys. Rev. Lett.* **73**, 1110 (1994).
[19] N. C. Lee and C. R. Choi, *Phys. Plasmas* **14**, 022307 (2007).
[20] P. H. Chavanis, *Phys. Rev. D* **76**, 023004 (2007).
[21] T. Katsouleas and W. B. Mori, *Phys. Rev. Lett.* **61**, 90 (1988).
[22] F. Haas, J. Goedert, L. G. Garcia and G. Manfredi, *Phys. Plasmas* **10**, 3858 (2003).
[23] B. Eliasson and P. K. Shukla, *J. Plasma Phys.* **76**, 7 (2009).
[24] R.Z. Sagdeev, *Rev. Plasma Phys.* **4**, 23 (1966).
[25] F. Verheest and M. A. Hellberg, *Electrostatic Solitons and Sagdeev Pseudopotentials in Space Plasmas: Review of Recent Advances*, in: "Handbook of Solitons: Research, Technology and Applications", Editors: S.P. Lang and S.H. Bedore, pp. 353-392 (Nova Science Publishers, Inc., 2009); ISBN 978-1-60692-596-6 2009.

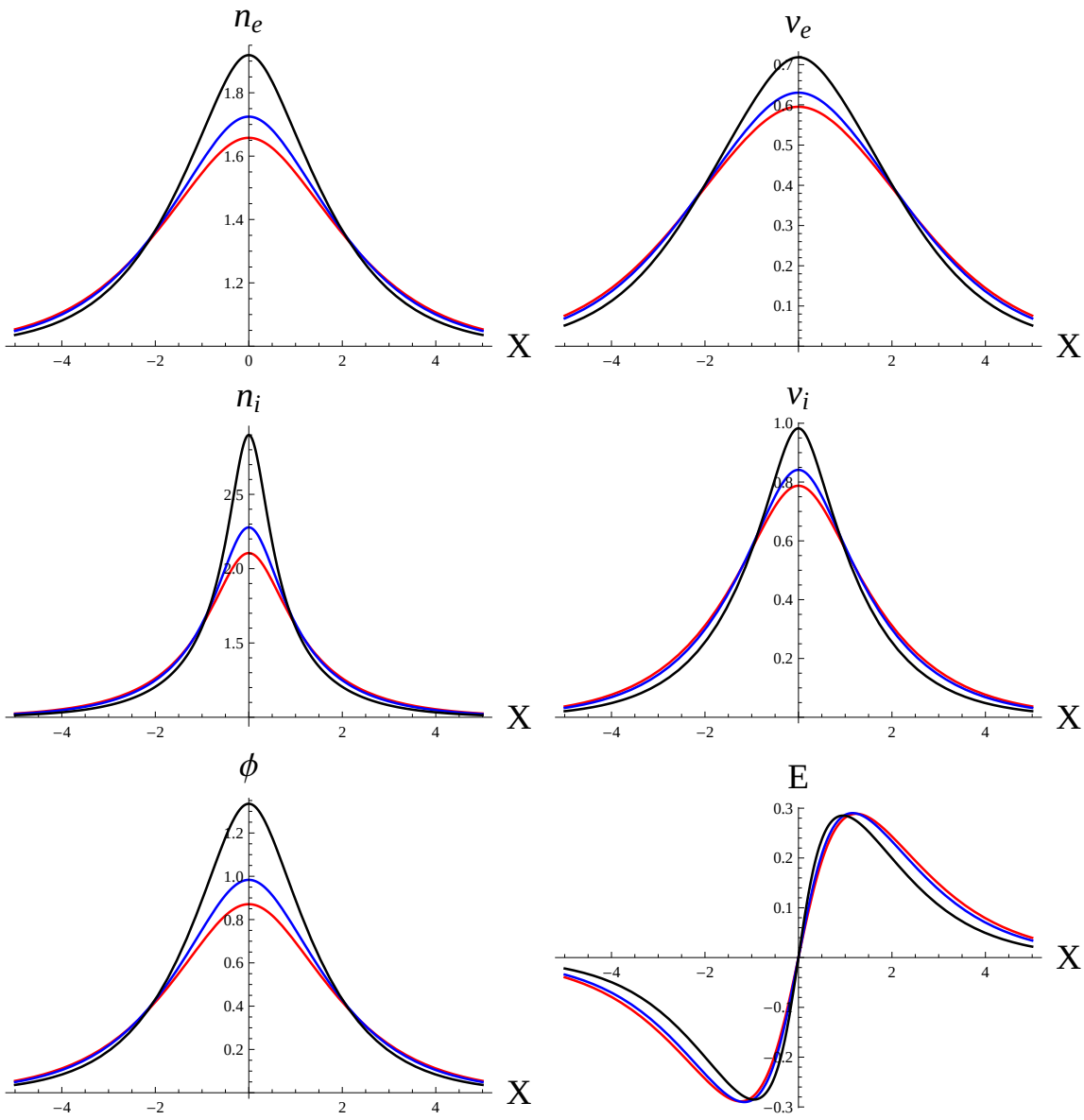

FIG. 6: (Color online) Plots of the plasma state variables are given, for different values of the electron density. Here, $M = 1.5$ throughout. With reference to the vertical axis at $X = 0$ (X=-4 in the graph for E), the upper (black), the middle (blue) and the lower (red) curves represent $n_0 = 10^{12}m^{-1}$, $5 \times 10^{11}m^{-1}$ and $10^{11}m^{-1}$ respectively.

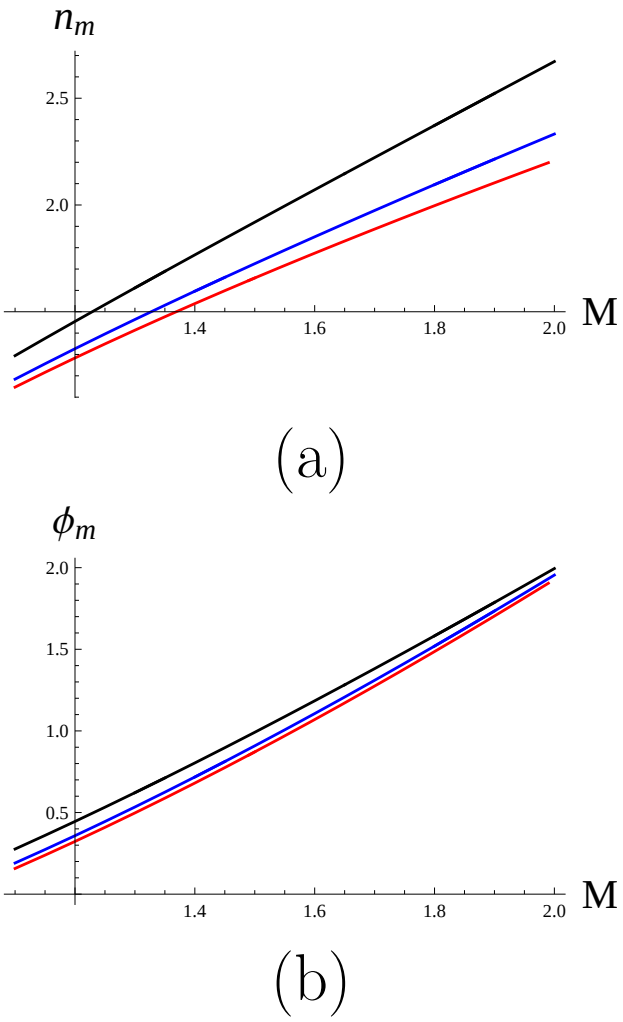

FIG. 7: (Color online) The amplitude (maximum value) of the electron-density (n_m) and potential (ϕ_m) excitations are plotted as functions of M, considering three values of n_0: upper (black)- $10^{12}m^{-1}$; middle (blue)- $5 \times 10^{11}m^{-1}$ and lower (red)-$10^{11}m^{-1}$.